Journal of Applied Electrochemistry **34**: 899–902, 2004.

Electrosynthesis of $Mg(OH)_2$ coatings on stainless steel substrates

M. DINAMANI and P. VISHNU KAMATH*
Department of Chemistry, Central College, Bangalore University, Bangalore 560 001, India
*(*author for correspondence, e-mail: vishnukamath8@hotmail.com)*

Received 24 November 2003; accepted in revised form 24 March 2004

Key words: cathodic reduction, DIFFaX simulation, electrosynthesis, magnesium hydroxide

Abstract

Cathodic reduction of aqueous solutions of $Mg(NO_3)_2$ results in the deposition of $Mg(OH)_2$ coatings on stainless steel cathodes. The coating growth is controlled by varying the deposition time, current density and the bath concentration. The coatings comprise thin scaly particles having sub-micron dimensions. DIFFaX simulations of the X-ray line broadening indicate the formation of small anisotropic particles having a thickness 134 Å measured along the [0 0 1] direction.

1. Introduction

A number of bivalent metal hydroxides, $M(OH)_2$ [M = Ca, Mn, Fe, Co and Ni] crystallize in the structure of mineral brucite, $Mg(OH)_2$ [1]. $Mg(OH)_2$ comprises a hexagonal packing of hydroxyl ions, in which the Mg^{2+} ions occupy alternative layers of octahedral sites. This results in a stacking of charge neutral metal hydroxide layers having the composition $[Mg(OH)_2]$. Besides the divalent hydroxides, several polymorphic modifications of $Al(OH)_3$ [2], a number of basic salts [3] and layered double hydroxides [4] also adopt structures derived from that of $Mg(OH)_2$.

$Mg(OH)_2$ has of late, acquired much importance because of its role in the mineral sequestration of CO_2, an important green house gas [5]. Besides, it undergoes thermal decomposition at a relatively low temperature (450 °C) to yield MgO, a material of industrial importance [6]. By varying the morphology and microstructure of the $Mg(OH)_2$ precursor, it is possible to control the morphology of nanoparticulate MgO [7]. $Mg(OH)_2$ has also been used as a sensor [8]. For many of these applications, $Mg(OH)_2$ has to be obtained in the form of thin/thick films or coatings.

Conventional techniques of thin film fabrication include pulsed laser deposition [9], rf sputtering [10], electron beam etching [11] and chemical vapor deposition [12]. All these techniques employ high power lasers, electron/ion beam sources as well as high temperatures making them inappropriate for application to low temperature phases such as $Mg(OH)_2$.

In this paper, we report the use of electrochemistry to obtain controlled growth of $Mg(OH)_2$ coatings on polycrystalline stainless steel (SS304) substrates. The synthesis of $Mg(OH)_2$ is described as a model system, which, in principle can be extended to the fabrication of coatings of other low temperature phases.

2. Experimental details

All $Mg(OH)_2$ coatings were prepared by the cathodic reduction of an aqueous magnesium nitrate (Merck) solution (concentration, 0.025–0.175 M) on a SS304 flag (surface area, 4.5 cm^2) in an undivided cell using a cylindrical Pt mesh (geometric area, 28 cm^2) as the counter electrode. All solutions were prepared using ion-exchanged (Barnstead Easypure™) water with a specific resistance of 18.3 MΩ cm. The synthesis was carried out in a galvanostatic mode using a Versastat Model II A (EG & G PARC) scanning potentiostat driven by M270 Software. The electrodeposition was carried out at current densities of 1 to 7 mA cm^{-2} for deposition times varying from 5 to 60 min. A saturated calomel electrode (SCE) was used as a reference electrode. After deposition, the working electrode was taken out of the bath, rinsed and dried to constant weight at 70 °C. The weight of the electrode with the coating was noted, the coating was washed off with dilute HNO_3 and the weight of the bare electrode was noted to monitor the coating growth.

Coatings were grown under different conditions and the coating weight monitored as a function of bath concentration, current density and deposition time. In all these experiments $Mg(OH)_2$ coatings were found to cover the substrate completely and did not peel off during rinsing, drying, weighing and sample preparation for diffraction and electron microscopy analysis.

Prior to electrodeposition, the working electrode was cleaned in detergent and electrochemically polished as described elsewhere [13]. The working electrode loses

Table 1. Atomic position parameters of $Mg(OH)_2$ used for DIFFaX simulation

Atom	Position coordinates			Occupancy factor
	x	*y*	*z*	
O	0.3333	0.6667	0.2190	1.00
Mg	0.0000	0.0000	0.0000	1.00
O	−0.3333	−0.6667	−0.2190	1.00

0.15–0.2 mg cm^{-2} during electrochemical polishing. It was observed that electrochemical polishing of the substrate improved the integrity of the coating and its bonding to the substrate. However, on prolonged electrodeposition (>60 min) the $Mg(OH)_2$ coating thickens, flakes off and collects at the bottom of the cell.

The coatings were characterized by X-ray diffractometry by directly mounting the electrode on a Siemens D5005 diffractometer operated in reflection geometry. Data were collected with CuKα ($\lambda = 1.541$ Å) radiation using a continuous scan rate of 1° min^{-1} at step size 0.02°. SEM studies were carried out using a JEOL JSM 840 Scanning Electron Microscope.

2.1. *PXRD simulation studies*

The Bragg peaks observed in the PXRD pattern of the $Mg(OH)_2$ coatings are considerably broadened. To investigate the origin of this broadening and to confirm if the pattern is indeed due to $Mg(OH)_2$, simulation studies were carried out using the Fortran based code DIFFaX [14]. Within the DIFFaX formalism, a solid is treated as a stacking of layers of atoms and the PXRD pattern is computed by integrating the diffraction intensity layer by layer. This formalism is ideally suited for a material such as $Mg(OH)_2$, where the layers naturally exist because of 2-dimensional bonding. The layers are stacked one on another according to a stacking vector. The use of vector (0,0,1) results in a crystalline lattice. The atomic position parameters used for the simulation are summarized in Table 1. The calculated Bragg maxima were broadened using a lorentzian line shape to account for instrumental broadening and other factors. A FWHM value of 0.4° in 2θ was chosen for the lorentzian to facilitate comparison with the experimental pattern, as it corresponds to the width of the sharpest reflection (1 1 0) in the observed pattern. For layered materials such as $Mg(OH)_2$, the crystallite size can be specified along the *a–b* plane as 'disc diameter' or along the *c*-axis as 'thickness'. Small disc diameters broaden the (1 1 0) reflection selectively [15] and therefore the broadening due to this factor is already accounted for in the lorentzian chosen. The value specified for the thickness was varied by hand, until a good visual match between the simulated and the experimental pattern was found. The 'goodness' of the match was estimated by comparing the FWHM of each reflection in the simulated pattern with that of its counterpart in the experimental pattern. A matching of the FWHMs within 0.1° in 2θ was considered satisfactory.

3. Results and discussion

$Mg(OH)_2$ has a low solubility product (10^{-12}) [16] which corresponds to a pH value of ~9.2. The conventional approach to $Mg(OH)_2$ synthesis would be chemical precipitation, wherein an aqueous Mg salt solution is made to react with a strong base such as NaOH. Other precipitating agents such as ammonia [17] could also be used. But in all these cases there is poor or no control over the precipitation kinetics, phase formation or crystal growth. Also bulk precipitation reactions such as these are not useful for the deposition of films and coatings.

Electrochemical reactions, on the other hand, take place at the electrode/electrolyte interface. Burke and coworkers [18] have grown hydrous oxide films by potentiodynamic cycling of reactive metal electrodes in an alkaline electrolyte. A typical example is the synthesis of mixed metal (Y, Ba, Cu) hydroxide film by cycling a copper foil electrode in baryta [19] containing dissolved salts of Y to obtain a film of the superconducting 123 phase. But this technique does not permit the solid state characterization of the film or a control over its growth.

To overcome this problem and facilitate the use of inert electrodes, we have employed the electrogeneration of base technique [20] based on the cathodic reduction of an aqueous solution of a suitable metal salt. The salt chosen in this study is $Mg(NO_3)_2$. Depending upon the deposition potential, choice of the anion and the pH of the solution, one or more of the following types of reactions [21] take place close to the cathode:

(i) reactions which consume H^+ ions,
(ii) electrolysis of water and
(iii) anion (nitrate) reduction reactions.

Of these the last type is considered the most significant [20]:

$$(a) NO_3^- + H_2O + 2e^- \rightarrow NO_2^- + 2OH^- \quad E^\circ = 0.01\ V$$
$$(b) NO_3^- + 7H_2O + 8e^- \rightarrow NH_4^+ + 10OH^-$$

All these reactions cause a steep increase in the pH of the solution close to the cathode, leading to the precipitation of $Mg(OH)_2$ according to the reaction:

$$Mg^{2+} + 2OH^- \rightarrow Mg(OH)_2 \downarrow$$

As the pH changes occur close to the electrode, the $Mg(OH)_2$ is deposited on the cathode. The deposit thickness can be controlled by varying the total charge passed and the rate of deposition can be varied by varying the cell current.

Indeed, within a few minutes of electrolysis, small white crystallites can be observed on the surface of the cathode. In Figure 1a, is shown the PXRD pattern of the coating. The observed *d*-spacings can be indexed on

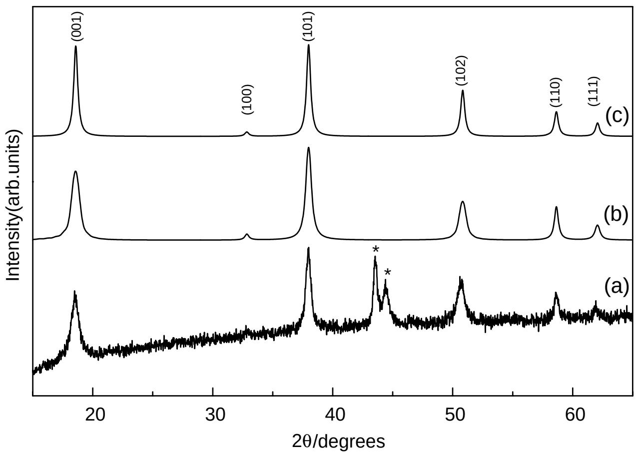

Fig. 1. (a) Observed powder X-ray diffraction pattern of $Mg(OH)_2$. (b) Simulated pattern incorporating particle size effects. (c) Simulated pattern without incorporating particle size effects. Features marked by the asterisks correspond to stainless steel peaks.

Table 2. Full width at half maximum (FWHM) values of the reflections observed in the PXRD pattern of a $Mg(OH)_2$ coating

hkl	FWHM (in degrees 2θ)	
	Observed	Simulated
001	0.8	0.82
101	0.6	0.59
102	0.8	0.79
110	0.4	0.42
111	0.5	0.61

a hexagonal cell (a = 3.15 Å; c = 4.77 Å) and match with those assigned to brucite-like $Mg(OH)_2$ (PDF: 7-238). To further confirm that the observed pattern is due to $Mg(OH)_2$, a DIFFaX simulation was carried out (see Figure 1c). Two notable differences are observed:

(1) The peaks corresponding to the various reflections in the observed pattern are non-uniformly broadened (see Table 2) and

(2) The relative intensities of the (0 0 1) and (1 0 1) reflections do not agree with the intensities computed by DIFFaX for crystalline $Mg(OH)_2$. In the observed pattern the (1 0 1) reflection is the most intense while in the simulated pattern the two have comparable intensities.

Line broadening is well known to arise due to particle size effects [22] and non-uniform broadening is attributed to anisotropic crystallite growth [23]. Further, particle size measured along the c-crystallographic axis is known to selectively affect the width and relative intensity of the (0 0 1) reflection [15]. Therefore, to simulate the broadening of the (0 0 1) reflection, the PXRD pattern was computed for a thickness of 28 layers (134 Å) (see Figure 1b). The resultant pattern was found to match well with the observed pattern. This simulation also generates the same degree of non-uniform broadening as in the observed pattern (Table 2). $Mg(OH)_2$ is a layered material, the successive hydroxide sheets are held by weak van der Waal's forces, while bonding in the a–b plane is covalent. Consequently, the microcrystalline domains are anisotropic with the planar dimension extending to micrometers while the thickness remains in the nanometer range. This anisotropy is the cause of the non-uniform broadening of the reflections in the PXRD pattern.

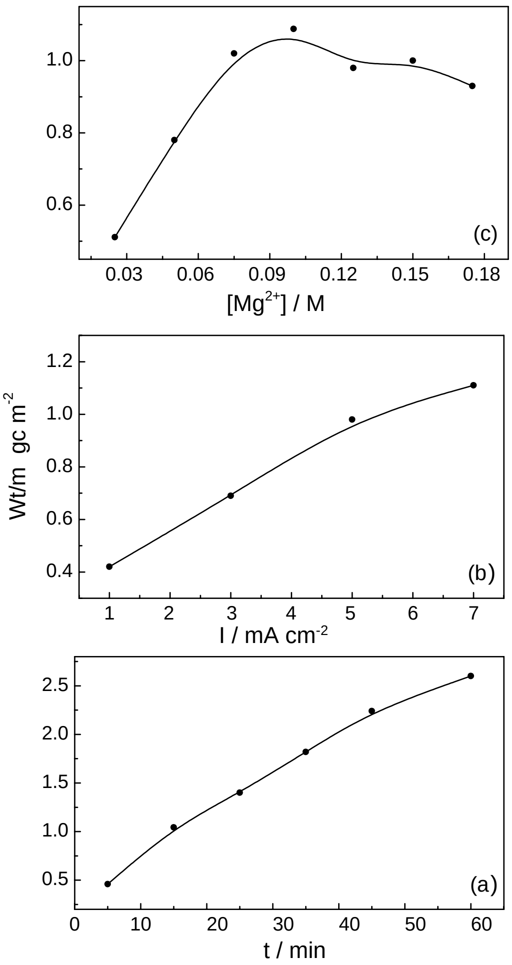

Fig. 2. Coating growth characteristics of $Mg(OH)_2$ as a function of (a) deposition time (bath concentration 0.1 M; current density 5 mA cm^{-2}), (b) current density (bath concentration 0.1 M; deposition time 15 m) and (c) concentration of the bath (current density 5 mA cm^{-2}; deposition time 15 m).

Figure 2 shows the coating growth characteristics of $Mg(OH)_2$ as a function deposition time, current density and bath concentration. Assuming a density of 2.36 g cm^{-3} [24] for $Mg(OH)_2$, the thickness of the deposit is estimated to vary from 1.7 to 11 μm depending on the amount of total charge (Q) passed during the deposition and the concentration of the bath. A limiting thickness of 4.3 ± 0.2 μm is achieved as a function of the bath concentration. Under other conditions the deposit thickens and flakes off and a limiting thickness could not be determined.

Scanning electron micrographs of $Mg(OH)_2$ at different magnifications are shown in Figure 3. At low magnifications, the substrate has been completely covered by a granular deposit of $Mg(OH)_2$. All the

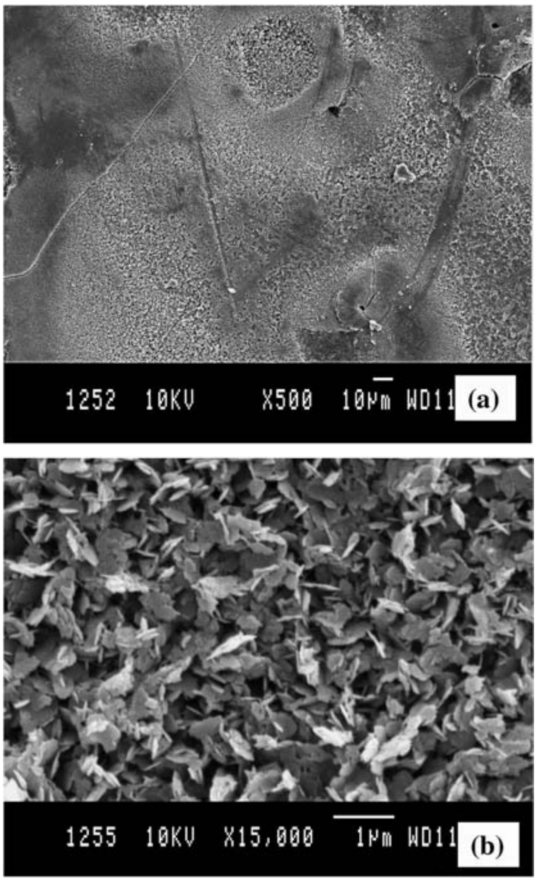

Fig. 3. Scanning electron micrographs of $Mg(OH)_2$ at (a) low and (b) high magnifications.

sub-millimeter scratches on the substrate have been covered over. At higher magnifications, the coating exhibits irregularly shaped flake-like morphology. The small domain size of the electrodeposits is evident as the flakes are of sub-micron dimensions. The needle shaped particles correspond to the flakes growing side-on over the substrate and thereby reveal the small thickness and the consequent anisotropy.

In conclusion, cathodic reduction of an aqueous $Mg(NO_3)_2$ solution enables the controlled growth of micrometer thick coatings of $Mg(OH)_2$ on conducting substrates. This is a general method that can be extended to any other metal hydroxide as well.

Acknowledgement

PVK thanks the University Grants Commission, Government of India (GOI) for the award of a Major Research Project. MD thanks the Council of Scientific and Industrial Research, GOI, for the award of a Senior Research Fellowship. The authors also thank the Solid State and Structural Chemistry Unit and the Department of Metallurgy, Indian Institute of Science for powder X-ray diffraction and electron microscopy facilities respectively.

References

1. H.R. Oswald and R. Asper, Bivalent Metal Hydroxides, *in* R.M. A. Leith (Ed), 'Preparation and Crystal Growth of Materials with Layered Structures' Vol. 1 (D.Reidel Publishing Company, Dordrecht, 1977) pp. 71–140.
2. H.D. Megaw, *Z. Krist.* **87** (1934) 185.
3. P.M. Louër, D. Louër, D. Grandjean and D. Weigel, *Acta. Cryst.* **B29** (1973) 1707.
4. F. Cavani, F. Trifiro and A. Vaccari, *Catal. Today* **11** (1991) 173.
5. M.J. McKelvy, R. Sharma, A.V.G. Chizmeshya, R.W. Carpenter and K. Streib, *Chem. Mater.* **13** (2001) 921.
6. S.H.C. Liang and I.D. Gay, *J. Catal.* **101** (1986) 293.
7. Y. Ding, G. Zhang, H. Wu, B. Hai, L. Wang and Y. Qian, *Chem. Mater.* **13** (2001) 435.
8. J.E. Moneyron, A. Deroy and J.-P. Besse, *Sensors Actuators* **B4** (1991) 189.
9. H. Yugami, H. Naito, H. Arashi and M. Ishigame, *Solid State Ionics* **86** (1996) 1307.
10. B.Y. Liaw, R.E. Rocheleau and Q.-H. Gao, *Solid State Ionics* **92** (1996) 85.
11. C. Byun, J.W. Jang, I.T. Kim, K.S. Hong and B.-W. Lee, *Mat. Res. Bull.* **32** (1997) 431.
12. M. Hartmanova, I. Thurzo, M. Jergel, J. Bartos, F. Kadlec, V. Zelezny, D. Tunega, F. Kundracik, S. Chromik and M. Brunel, *J. Mater. Sci.* **33** (1998) 969.
13. D.A. Corrigan and R. M. Bendert, *J. Electrochem. Soc.* **136** (1989) 723.
14. M.M.J. Treacy, M.W. Deem and J.M. Newsam, Computer Code DIFFaX, Version 1.807.
15. T.N. Ramesh, R. S. Jayashree and P.V. Kamath, *Clays and Clay Minerals* **51** (2003) 570.
16. D. Dobos, 'Electrochemical Data' (Elsevier, Amsterdam, 1975) p. 221
17. T.N. Ramesh, M. Rajamathi and P.V. Kamath, *Solid State Sci.* **5** (2003) 751.
18. L.D. Burke and M.E.G. Lyons, *in* R.E. White et al. (Eds.) 'Modern Aspects of Electrochemistry 18' (Plenum Press, NY 1986) p. 169.
19. D.J. Zurawski, P.J. Kulesza and A. Wieckowski, *J. Electrochem. Soc.* **135** (1988) 1607.; P. Slezak and A. Wieckowski, *J. Electrochem. Soc.* **138** (1991) 1038.
20. J.A. Switzer, *Am. Ceram. Soc. Bull.* **66** (1987) 1521.
21. Y. Matsumoto, T. Morikawa, H. Adachi and J. Hombo, *Mat. Res. Bull.* **27** (1992) 1319.
22. A.R. West, 'Solid State Chemistry and its Applications' (John Wiley and Sons, Singapore 1987) p. 173
23. M.C. Bernard, R. Cortes, M. Keddam, H. Takenouti, P. Bernard and S. Senyarich, *J. Power Sources* **63** (1996) 247.
24. R.C. Weast (Ed.), 'The Hand book of Chemistry and Physics', (Chemical Rubber Co., Cleveland, 1986).